

Wear Characteristics of Ni-Based Hardfacing Alloy Deposited on Stainless Steel Substrate by Laser Cladding

REENA AWASTHI, P.K. LIMAYE, SANTOSH KUMAR, RAM P. KUSHWAHA, C.S. VISWANADHAM, DINESH SRIVASTAVA, N.L. SONI, R.J. PATEL, and G.K. DEY

In this study, dry sliding wear characteristics of the Ni-based hardfacing alloy (Ni-Mo-Cr-Si) deposited on stainless steel SS316L substrate by laser cladding have been presented. Dry sliding wear behavior of the laser clad layer was evaluated against two different counter bodies, AISI 52100 chromium steel (~850 VHN) and tungsten carbide ball (~2200 VHN) to study both adhesive and abrasive wear characteristics, in comparison with the substrate SS316L using ball on plate reciprocating wear tester. The wear resistance was evaluated as a function of load and sliding speed for a constant sliding amplitude and sliding distance. The wear mechanisms were studied on the basis of wear surface morphology and microchemical analysis of the wear track using SEM-EDS. Laser clad layer of Ni-Mo-Cr-Si on SS316L exhibited much higher hardness (~700 VHN) than that of substrate SS316L (~200 VHN). The laser clad layer exhibited higher wear resistance as compared to SS316L substrate while sliding against both the counterparts. However, the improvement in the wear resistance of the clad layer as compared to the substrate was much higher while sliding against AISI 52100 chromium steel than that while sliding against WC, at the same contact stress intensity.

DOI: 10.1007/s11661-014-2719-x

© The Minerals, Metals & Materials Society and ASM International 2014

I. INTRODUCTION

WEAR and corrosion are the most frequently encountered surface-initiated failure mechanisms for components working under aggressive conditions. Since these failures always initiate at the surface, therefore, it is economical and effective to modify the surface of the components without affecting the bulk, using suitable surface modification methods. Laser cladding is an advance surface modification technology, which has the capability of applying advanced coating materials with low dilution and rapidly solidified microstructure. Laser cladding technique has the advantage of depositing a controlled thickness of the clad material on a selected area of the substrate. Various studies have shown superior characteristics of the hardfacing alloys deposited by laser cladding as compared to other conventional surfacing techniques.^[1-4] Cobalt and nickel-based Triballoys, a family of intermetallic alloys, have been developed as wear and corrosion-resistant material over a wide range of temperatures and environments.^[5] Triballoy series of alloys are characterized by the presence of a large volume fraction of a hard intermetallic Laves phase

in a much softer solid solution or a eutectic phase mixture.^[6-10] Laves phase strengthened alloys are not only very hard but also rather brittle; therefore, these alloys are most commonly applied as a coating.^[11,12] The high cost, scarcity, and non-suitability of Co-based alloys in nuclear industries due to induced activity led to the development of nickel and iron-based alloys to replace cobalt-based hardfacing alloys.^[13,14] A nickel-based alloy Ni-32 wt pctMo-15 wt pctCr-3 wt pctSi (Triballoy T-700) exhibited better wear performance than several stainless steels and other nickel-based counterparts.^[15,16] These alloys have been described as an alternative to the cobalt-based Triballoy for nuclear applications involving wear, corrosion, and high temperature oxidation.^[17,18] Wear behavior of the welded, laser clad, or thermally sprayed Co-based (Co-Mo-Cr-Si) triballoy series of alloys^[19-22] has been studied extensively. However, the literatures on wear behavior of the laser-deposited Ni-based (Ni-Mo-Cr-Si) triballoy series of alloy are limited.^[16] Kumar *et al.*^[16] have reported the wear behavior of the laser-deposited Ni-based clad layer on mild steel substrate as compared to that of stellite-6 layer against 600 grit sized SiC abrasive paper, using pin on disk method. The Ni-Mo-Cr-Si laser clad layer displayed better abrasive wear resistance as compared to the most popular Co-based hardfacing material stellite-6 alloy. Bolelli *et al.*^[23] have reported the wear characteristic of thermally sprayed Ni-Mo-Cr-Si Triballoy alloy under wider range of dry sliding contact conditions by rotating unidirectional ball on disk method. In this study, the wear behavior of the High velocity oxygen-fuel-sprayed (HVOF) Co-based Triballoy-800 coating has been compared to the Ni-based Triballoy-700 by ball-on-disk tests against different

REENA AWASTHI, SANTOSH KUMAR, and DINESH SRIVASTAVA, Scientific Officers, RAM P. KUSHWAHA, Technical Officer, and G.K. DEY, Head, are with the Materials Science Division, Bhabha Atomic Research Centre, Mumbai, India. Contact email: reena@barc.gov.in P.K. LIMAYE, N.L. SONI, and R.J. PATEL, Scientific Officers, are with the Refueling Technology Division, Bhabha Atomic Research Centre. C.S. VISWANADHAM, Scientific Officer, is with the Nuclear Controls and Planning Division, Department of Atomic Energy, Mumbai, India.

Manuscript submitted May 13, 2014.

Article published online January 7, 2015

counter bodies (100Cr6 steel and sintered alumina). HVOF-sprayed Tribaloy coatings exhibited a layered lamellar microstructure due to high velocity impact of heated particles. While in our previous investigation,^[9,10] laser-clad Triballoys displayed a fully crystalline fine microstructures, resulting from rapid melt solidification. Therefore, the studies on wear characteristics of HVOF-sprayed coatings cannot be directly correlated to welded or laser clad Triballoys coatings. Further, it is also not relevant to directly compare the present results with the reported^[23] wear characteristics of HVOF-sprayed (Ni-Mo-Cr-Si) tribaloy, because of different sliding wear techniques and the wear conditions.

Detailed studies on wear characteristics of the laser-deposited Ni-based (Ni-Mo-Cr-Si) tribaloy series of alloy are scarce. In the present study, the wear resistance of the clad layer was evaluated using reciprocating wear test against two different counter bodies, AISI 52100 chromium steel (~850 VHN) and tungsten carbide (~2200 VHN) balls. The wear studies of SS316L (~200 VHN) and Ni-Mo-Cr-Si (700 VHN) laser clad layer sliding against 52100 Cr steel ball (~850 VHN) fall under the adhesive wear regime because of chemical compatibility (metallic) and closer hardness of both the counterparts. While due to much higher hardness (~2200 VHN) and chemical incompatibility between the ceramic WC ball and metallic surfaces of the laser clad layer and substrate, the wear regime is abrasive in nature when sliding against WC counterpart is considered. A wider range of dry sliding contact condition (load and speeds) was studied using ball on plate reciprocating wear test method. The sliding wear mechanisms are discussed based on wear surface morphology by SEM-EDS analysis. Detailed investigation on the wear characteristics of Ni-Mo-Cr-Si alloy deposited on SS316L using Nd: YAG laser is reported and compared to the reference substrate SS316L.

II. EXPERIMENT

A Ni-based alloy powder having composition Ni-32 pctMo-15 pctCr-3 pctSi (wt pct) and a particle size range of ~50 to 80 μm with spherical morphology was deposited on stainless steel 316L substrate (dimension: 25 mm \times 20 mm \times 10 mm) using laser cladding method. The laser cladding was conducted using 1 KW Nd:YAG laser equipped with co-axial powder feed nozzle. The laser cladding parameters (laser power: 800 W, powder feed rate: 8.3 gm/min, scanning speed: 200 mm/min, spot size: 2 mm) were optimized to obtain defect free, metallurgically bonded, and low diluted clad layer on SS316L substrate. Multiple tracks were clad side by side with approximately 50 pct overlap between adjacent tracks in order to cover the whole surface. The microstructure of the clad layer was analyzed by Scanning electron microscope attached with Energy dispersive spectroscopy. The phases were identified by X-Ray Diffraction with Cu K α radiation. The average hardness was taken by a Vickers microhardness tester using 10 N load at the surface of the sample.

The dry sliding wear resistance of the laser clad layer surface was evaluated against two different counter bodies, AISI 52100 chromium steel ball with nominal hardness (~850 VHN) and WC ball (~2200 VHN), using ball on plate reciprocating wear tester. The average initial hertzian contact stress intensity was kept same for both the counterparts. The wear test was performed on the microfriction machine (TE 70 Plint) at room temperature. The substrate SS316L was also evaluated as a reference material for comparison. Wear tests were carried out on the polished specimen (average roughness of 0.2 μm) at room temperature without lubrication. As shown schematically in Figure 1, the ball (counter body) of specific diameter slides (at particular speed) over the plate (specimen) under load. The ball (WC and 52100 Cr steel) was made to slide on the plate (samples) at various load and sliding speeds as shown in Table I, keeping the sliding amplitude of 1 mm and sliding distance of 100 m constant. The friction coefficient was recorded as a function of sliding cycles during the test. The wear volume was calculated by integrating the area of the wear scar profile over the entire length of the wear scar, measured by 3-D profilometry (Figure 2). The wear morphologies and the involved wear mechanisms were studied by scanning electron microscopy with energy dispersive spectroscopy (SEM-EDS).

III. RESULTS

A. Microstructure

The laser clad layer of Ni-Mo-Cr-Si alloy (thickness ~1 mm) was metallurgically bonded with the substrate SS316L, shown in the cross-sectional micrograph (Figure 3(a)). The clad surface layer exhibited a uniform microstructure consisting of primary dendrites of Mo-rich phase dispersed in softer Ni-based gamma solid solution or lamellar eutectic phase mixture of both (Figure 3(b)). The clad layer at the surface exhibited low dilution (~11 pct) confirmed by EDS. X-ray diffraction analysis (Figure 4) carried on the surface of the clad

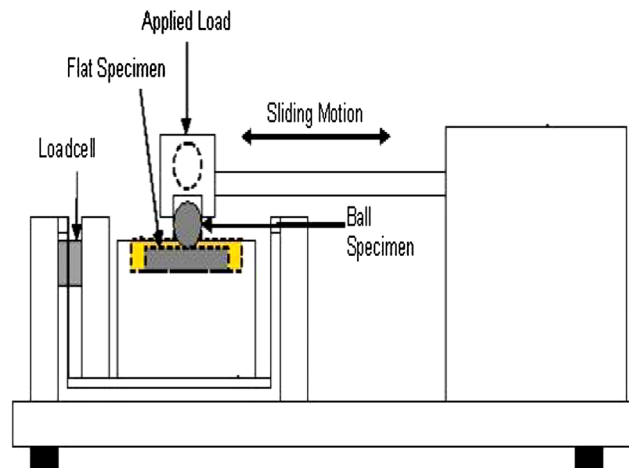


Fig. 1—Schematic of the reciprocating wear test.

Table I. Reciprocating Sliding Wear Test Conditions

Ball Material	WC Ball						Cr Steel Ball					
Load (N)	3	5	7	5	5	5	3	5	7	5	5	5
Sliding frequency (Hz)	10	10	10	10	20	30	10	10	10	10	20	30
Speed (mm/s)	20	20	20	20	40	60	20	20	20	20	40	60

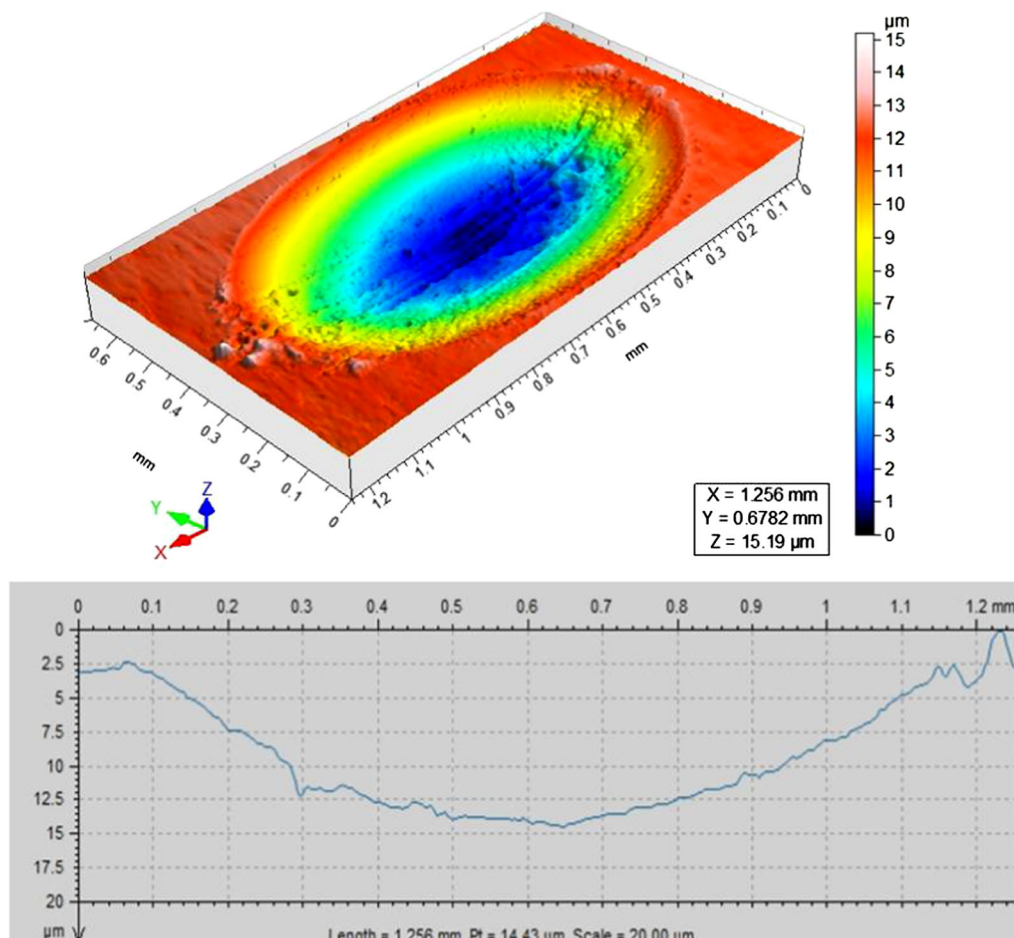


Fig. 2—Typical 3-D profilometry view of the sample.

layer, indicated the presence of primary hexagonal close-packed (hcp) intermetallic Laves phase dispersed in gamma solid solution with face-centered cubic crystal structure. The average hardness of clad layer (~700 VHN) was higher in comparison to that of the SS316L substrate (~200 VHN).

B. Wear Studies Using AISI 52100 Cr Steel Ball as the Counter Body

1. Wear properties

The laser clad layer exhibited significantly higher wear resistance as compared to the SS316L as the volume loss was much lower in case of clad than SS316L under all the loading conditions (Figure 5(a)). Both substrate and clad layer showed a linear increase in the wear volume

with the increasing load (Figure 5(a)) which showed that the wear law was followed. From this relationship, the wear rate (mm^3/Nm) of the both the materials was calculated according to Archard's relationship for wear law.^[24] The wear rate of the clad layer (1.864 to $4.635 \times 10^{-6} \text{ mm}^3/\text{Nm}$) was lower (~4 to 5 times) than substrate SS316L (0.666 to $1.711 \times 10^{-5} \text{ mm}^3/\text{Nm}$) at various loading conditions. Although the wear rate of the clad as well as the substrate increased with increasing load, the initial rate of increase was sharper in the substrate than that in the clad layer (Figure 5(b)). The wear rate of the substrate showed steep increase indicating transition from mild wear to severe wear, whereas wear rate of clad showed gradual linear increase, indicating significantly mild wear regime.

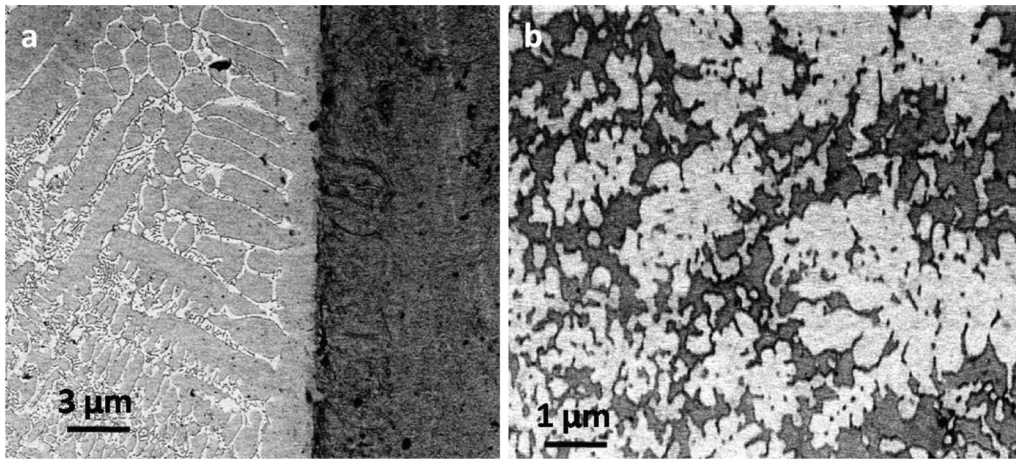


Fig. 3—(a) Metallurgical bonding to the substrate (b) microstructure of the clad layer.

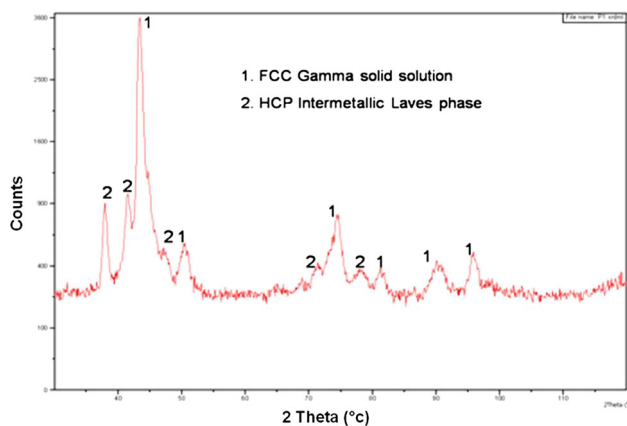


Fig. 4—X-ray diffraction pattern for laser clad layer of Ni-Mo-Cr-Si alloy.

The clad layer exhibited substantially lower volume loss as compared to the substrate SS316L at all speeds (Figure 5(c)). With increase in the speed, the wear rate of both the materials increased in similar manner, sharper in the initial part and flattened subsequently. An improvement of 2 to 5 times was observed in the wear rate of the laser clad layer (3.091 to 10.5×10^{-6} mm³/Nm) at various speeds as compared to that of the substrate SS316L (1.444 to 2.139×10^{-5} mm³/Nm). The wear rate of the 52100 Cr steel ball was also found to be lower (2.763×10^{-7} to 2.260×10^{-6} mm³/Nm) in sliding against the laser clad layer as compared to the substrate SS316L (2.326×10^{-6} to 1.353×10^{-5} mm³/Nm) at various loads as well as the speeds under the present study.

The coefficient of friction (COF) as a function of sliding distance for the laser clad layer and the substrate SS316L under identical test conditions of normal load 5 N and sliding speed of 20 mm/s is shown in Figure 6. The COF of substrate increased with time in the initial sliding to a maximum value of 0.27 ± 0.002 and then slightly reduced and stabilized at 0.25 throughout the entire sliding. Similarly, the COF of clad layer increased

to a value of 0.28 ± 0.006 and rose to a stable value ranging between 0.32 and 0.34. Small discrete oscillation in COF between 0.24 and 0.34 was noticed, which may be attributed to ejection of wear debris from the contact area. Average stabilized values of coefficient of friction were determined from these graphs. Average COF was found to increase with an increase in load for both the substrate (0.12 to 0.30) and clad layer (0.29 to 0.52).

2. Worn surface morphology

In order to understand the wear mechanism, worn surfaces were examined by SEM-EDS. The SEM micrographs of the middle of the wear track of the substrate SS316L under different loads along with the EDS analysis are shown in Figure 7. The wear track displayed considerable damage with the evidence of plastic deformation and shearing indicating adhesive wear at all loading conditions. Small dips (1 in Figures 7(a) through (c)) in the damaged area indicated that substrate might have adhered to the 52100 Cr steel ball counterpart. In some of the damaged areas, detachment of the material (marked 2 in Figure 7(b)) was observed. Some areas of the wear track were also found to be oxidized (Figure 7(d)). The wear track at different loads did not exhibit significant morphological differences (Figures 7(a) through (c)). With increasing load, the severity of damage increased in terms of amount of wear debris and brittle detachment of material (2 in Figures 7(b), (c)). The compacted wear debris (Figure 7(e)) found at the centre of the track consisted of small agglomerated rounded particle primarily consisting of Fe and O. Transfer of material and parallel longitudinal grooves can be clearly seen in the wear track of 52100 Cr steel ball track (Figure 7(f)).

Similar mechanisms of adhesive wear, deformation of surface, shearing, and material detachment due to cyclic plastic yielding were observed at all the speeds (Figures 8(a) through (c)). The residual oxide was found inside the wear track (Figure 8(d)). Thus, wear of the substrate proceeded from combined action of adhesion and transfer of material, plastic deformation, as well as oxidation and consequent delamination of the layer.

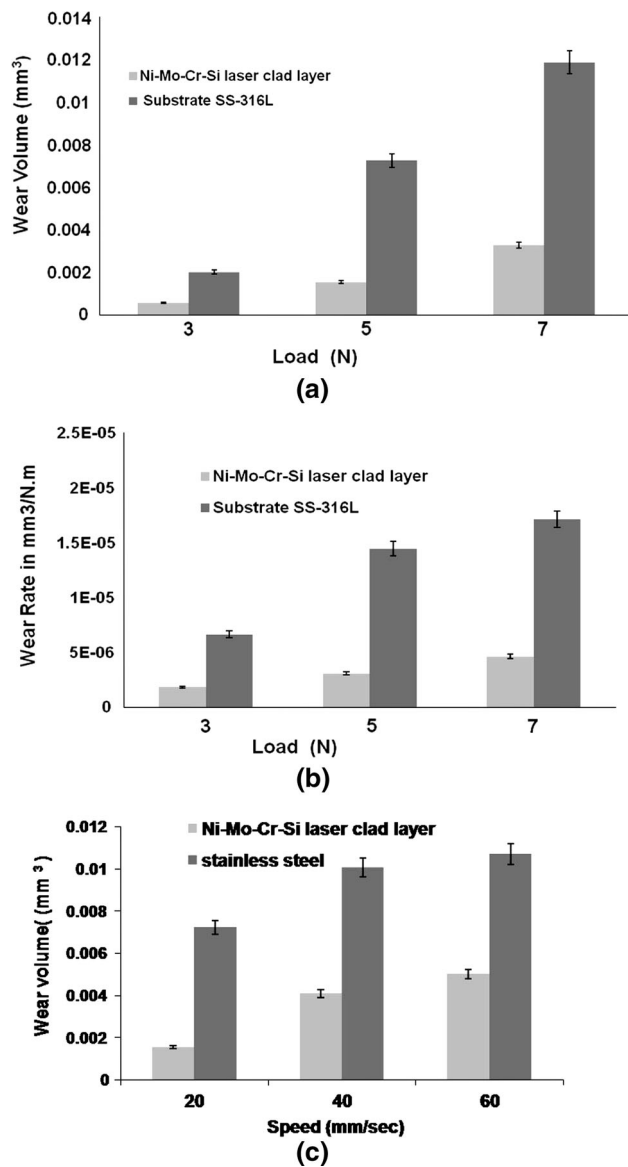


Fig. 5—(a) Variation of the wear volume vs load (constant speed 20 mm/s) for the Ni-Mo-Cr-Si laser clad layer and SS316L substrate sliding against 52100 Cr steel ball. (b) Variation of the wear rate vs load (constant speed 20 mm/s) for the Ni-Mo-Cr-Si laser clad layer and SS316L substrate sliding against 52100 Cr steel ball. (c) Variation of the wear volume vs speed (constant load of 5 N) for the Ni-Mo-Cr-Si laser clad layer and SS316L substrate sliding against 52100 Cr steel ball.

The wear track of laser clad layer did not display much damage at lower loads up to 5 N. No evidence of plastic shearing, adhesive wear (Figures 9(a), (b)), and oxidation (Figure 9(c)) was observed up to 5 N load. The worn surface was so smooth that the microstructure features were clearly revealed (Figure 9(c)). But as the load increased to 7 N, the wear track displayed layer-like transfer of material and microcracks (Figure 9(d)). The presence of discontinuous oxide film consisting of all the elements of the clad materials and high iron (Figure 9(e)) was also observed at higher load of 7 N. High Iron content indicated transfer of material from the 52100 Cr steel ball. The material transferred to 52100 Cr

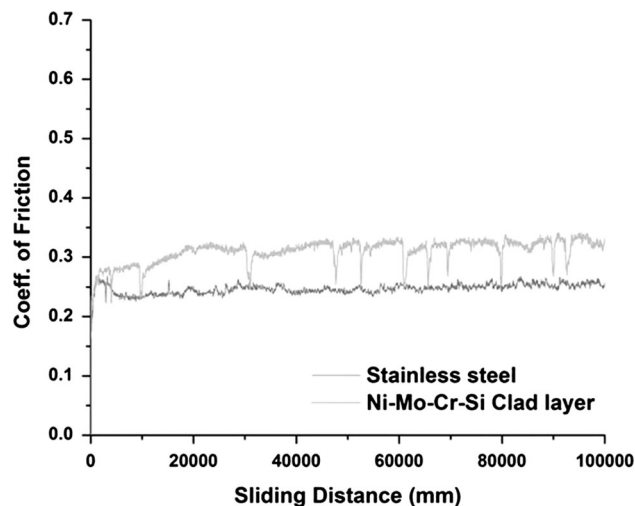


Fig. 6—Coefficient of friction vs sliding distance for the Ni-Mo-Cr-Si laser clad layer and SS316L substrate sliding against 52100 Cr steel ball (5 N, 20 mm/s).

steel ball, strain hardened, and consequently delaminated at certain location in wear track of the ball under high load (Figure 9(f)).

The wear track of clad layer sliding under the lowest speed of 20 mm/s did not display much damage, either plastic deformation or oxidation (Figure 10(a)). But as the speed increased, the wear mode changed to transfer of material, oxidation, and consequent cracking and delamination of layer (Figures 10(b), (c)). Discontinuous oxide layer (Figure 10(d)) consisted of high Fe (33 wt pct) and O with the other constituent elements of the clad material. High Fe content indicated wear of the steel counterpart and transfer to the coating. The wear debris from steel counterpart contributed to the oxidation of the wear track and consequent material detachment. Wear debris at the edges of the wear track was mainly found at higher sliding speeds. This debris consisted of both large and small wear particles of rounded morphology (Figure 10(f)).

Thus, the clad layer is highly resistant to wear (as inferred by the lack of any indication of plastic deformation, adhesion, or oxidation) up to a load 5 N and speed of 20 mm/s. The wear mode of the clad layer at higher load and higher speed (beyond 40 mm/s) was oxidation and consequent delamination of the discontinuous oxide layer.

C. Wear Studies Using a Tungsten Carbide Ball as the Counter Body

1. Wear properties

The wear volume of clad layer was smaller than that of the substrate SS316L at all loading conditions (Figure 11(a)). The volume loss increased with the increasing load in both the materials. Thus, wear law was obeyed in this case as well. Wear rate of the laser clad layer (~ 1.48 to 1.55×10^{-4} mm³/Nm) was found to be approx 1.5 times lower as compared to that of the SS316 L (2.08 to 2.29×10^{-4} mm³/Nm) at all loading conditions (Figure 11(b)). The wear rate of the laser clad

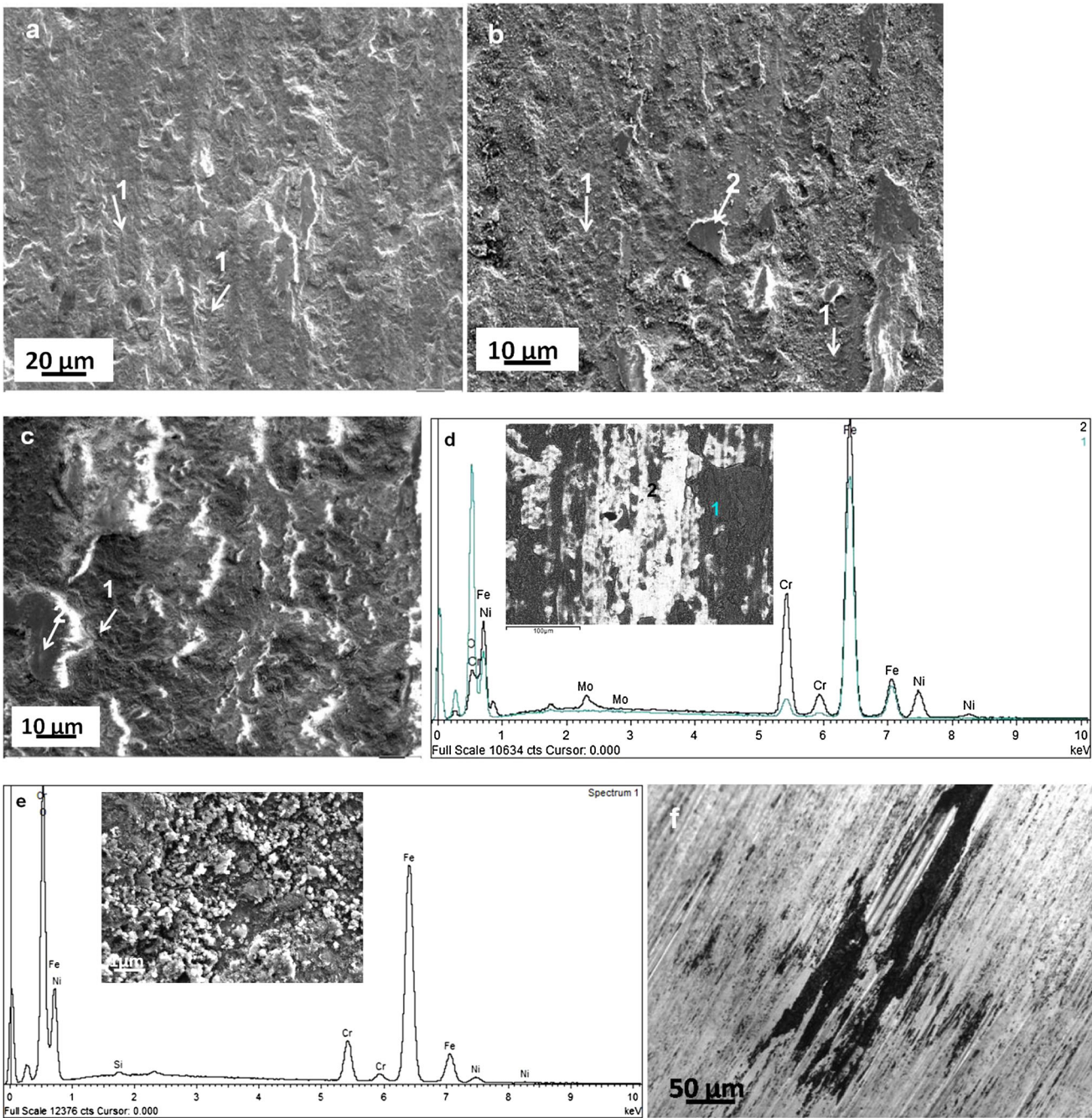


Fig. 7—SEM micrographs showing the morphology of the middle of wear track of the substrate SS316L under different loads (constant speed 20 mm/s) sliding against Cr steel ball (a) 3 N (b) 5 N (c) 7 N (d) BSE image and EDS microanalysis of the wear track (e) wear debris and EDS microanalysis (f) wear track of the Cr steel ball.

layer as well as SS316L was found to be nearly constant with the increasing load.

The clad layer exhibited marginally lower wear than SS316L only at lower speed of 20 mm/s. But as the speed increased, there were no appreciable differences in the wear volume of both the materials. Wear rates of the clad layer (~ 1.55 to 2.39×10^{-4} mm³/Nm) were not appreciably lower than those of SS316L (2.08 to 2.57×10^{-4} mm³/Nm) except at lower speed of 20 mm/s where the wear rate of clad is nearly 1.5 times

lower than that of SS316L. The wear rate of the ball sliding against the clad layer was found to be higher in the range of 3.17×10^{-6} to 5.08×10^{-6} mm³/Nm at various loading conditions, whereas for SS316L it was in the range of 2.78×10^{-7} to 9.92×10^{-7} mm³/Nm.

The coefficient of friction as a function of sliding distance for laser clad layer and the substrate SS316L sliding against WC ball under identical test conditions (normal load 5 N and sliding speed of 20 mm/s) is shown in Figure 12. The COF of the substrate increased

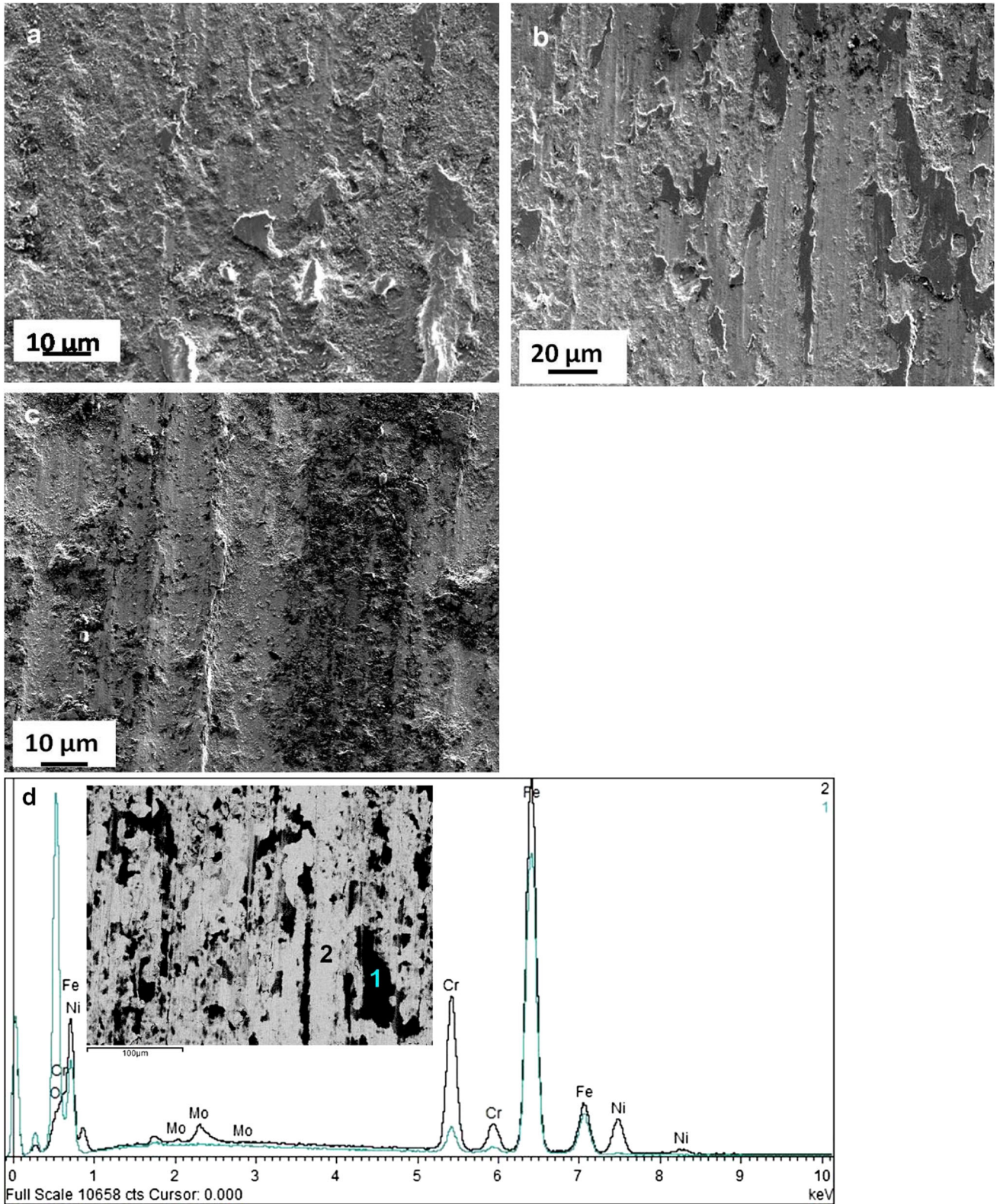


Fig. 8—SEM micrographs showing the morphology of the middle of wear track of the substrate SS316L under different speeds (constant load 5 N) sliding against Cr steel ball (a) 20 mm/s (b) 40 mm/s (c) 60 mm/s (d) BSE image and EDS microanalysis of wear track.

during initial sliding to a maximum value of 0.5 ± 0.012 and then slightly reduced to a value of 0.45 before stabilizing at 0.5 throughout the sliding distance. The

coefficient of friction of the clad layer displayed large oscillations in COF ranging between 0.45 and 0.60 throughout the sliding. Average COF showed marginal

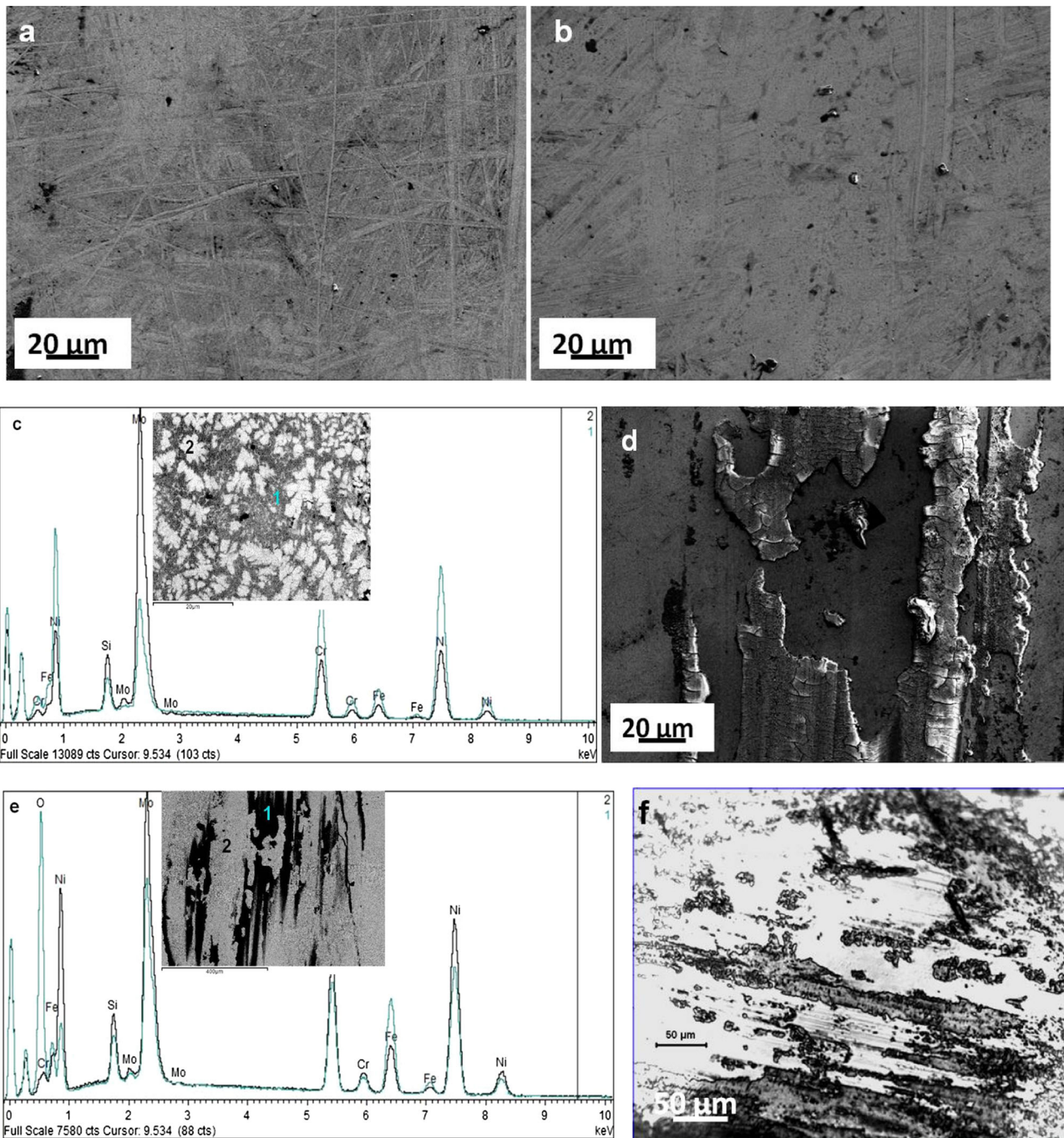


Fig. 9—SEM micrographs showing the morphology of wear track of the Ni-Mo-Cr-Si laser clad layer under different loads (constant speed 20 mm/s) sliding against Cr steel ball (a) 3 N (b) 5 N (c) BSE image and EDS microanalysis at 5 N (d) SEM at 7 N (e) BSE image and EDS microanalysis at 7 N and (f) wear track of the Cr steel ball.

reduction with increase in load for both the substrate (0.56 to 0.48) and clad layer (0.65 to 0.46).

2. Worn surface morphology sliding against tungsten carbide ball

The wear track of the substrate SS316L displayed parallel abrasion grooves in some of the damaged area, whereas in other areas of the track a layer of the transferred material is clearly visible in all the contacting

conditions (Figures 13(a) through (c)). The high level of oxygen confirmed the oxidized state of this layer (Figure 13(d)) consisting of high W (~32 to 35 wt pct) from the counterpart wear and also other constituents of the stainless SS316L at all loading and speed conditions. The oxide layer displayed cracking and brittle fracture. The wear track displayed similar wear mechanism in all contacting conditions (Figures 13(a) through (c)). Wear debris mostly segregated at the edges (at higher loads

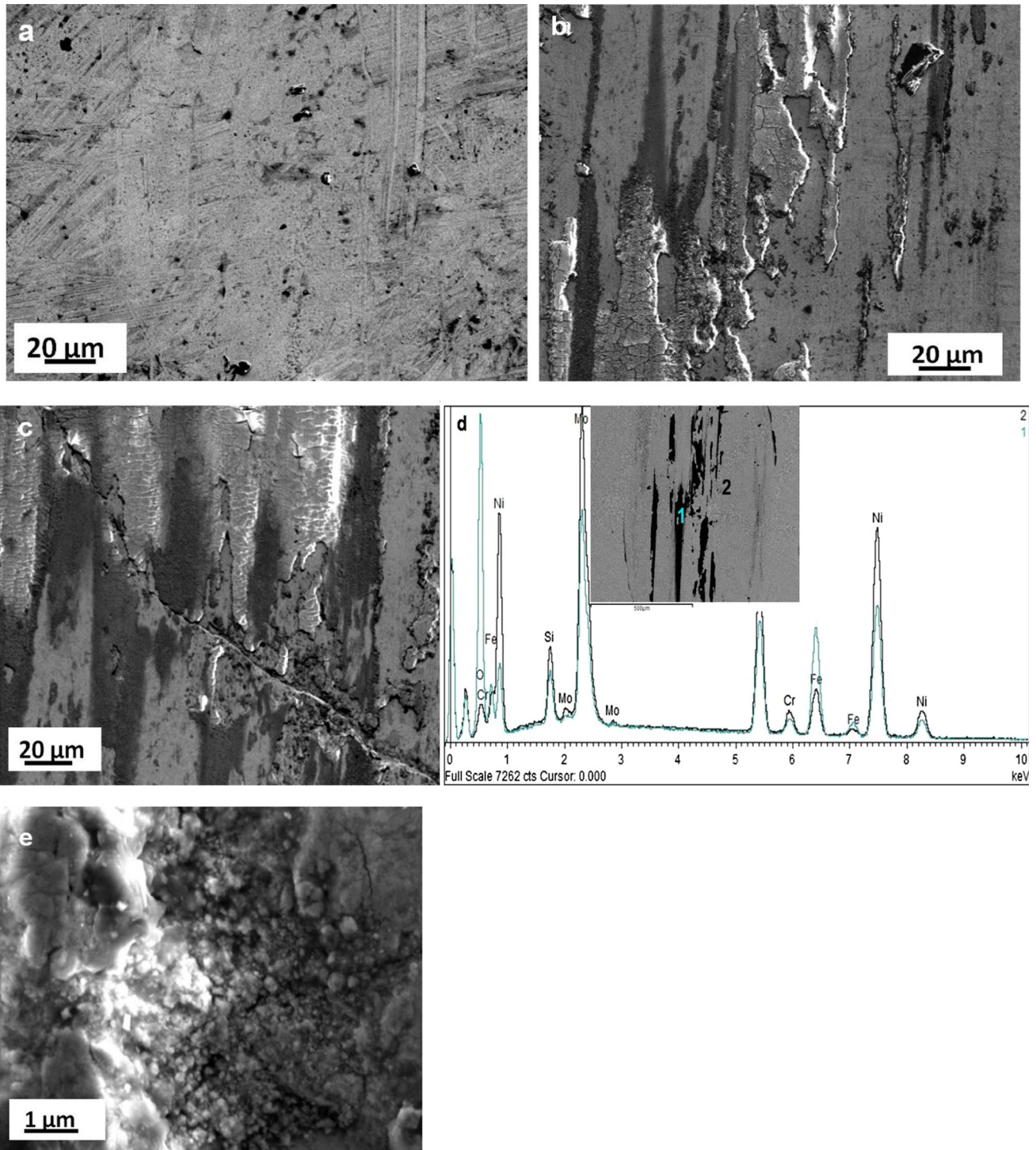


Fig. 10—SEM micrographs showing the morphology of the middle of wear track of the Ni-Mo-Cr-Si laser clad layer under different speeds (constant load 5 N) sliding against Cr steel ball (a) 20 mm/s (b) 40 mm/s (c) 60 mm/s (d) BSE image and EDS microanalysis of wear track (e) morphology of wear debris.

and speed) of the track consisted of mixture of both large and compacted small rounded particle primarily consisting of Fe with little W and O (Figure 13(e)). Transfer of material from the substrate and shallow grooves caused by entrapped WC wear particles can be clearly seen in the wear track of the ball (Figure 13(f)).

Similar wear mechanisms of abrasion as well as transfer of material and its oxidation with consequent brittle fracture were observed at all sliding speeds (Figures 14(a) through (c)). The discontinuous oxide clusters were also observed at some of the location of the track (Figure 14(d)).

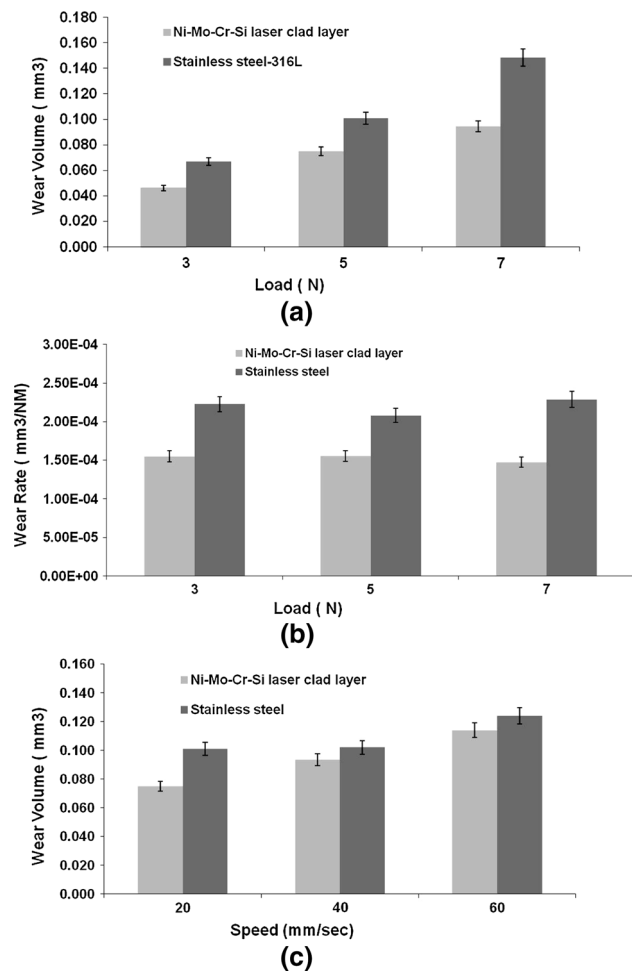


Fig. 11—(a) Variation of the wear volume vs load (constant speed 20 mm/s) for the Ni-Mo-Cr-Si laser clad layer and SS316L substrate sliding against WC ball. (b) Variation of the wear rate vs load (constant speed 20 mm/s) for the Ni-Mo-Cr-Si laser clad layer and SS316L substrate sliding against WC ball. (c) Variation of the wear volume vs speed (constant load 5 N) for the Ni-Mo-Cr-Si laser clad layer and SS316L substrate sliding against WC ball.

The wear track of clad layer exhibited shallow and smooth surface with very little deformation at low load of 3 N (Figure 15(a)). At higher load (Figures 15(b), (c)), the wear mode changed to initiation of microcrack from wear mode of low deformation at lower loads. But still no evidence of delamination of the clad layer was seen. High oxygen content (dark contrast) indicated the oxidized state consisting of all constituent of the clad material with very little W (1.5 to 2 wt pct), whereas brighter region indicated no oxidation and consisted of all the constituents of the clad with higher Mo content than that in the darker area (Figure 15(d)). Some amount of Fe present was due to small dilution of the clad layer with SS316L substrate. The wear debris mostly present at higher load of 7 N (Figure 15(f)) was composed of very fine compacted particle consisted of all the constituent elements of the clad layer.

Similar mechanism of low deformation and oxidation was observed at low speed of 20 mm/s (Figure 16(a)), whereas microcracking and oxidation at still higher

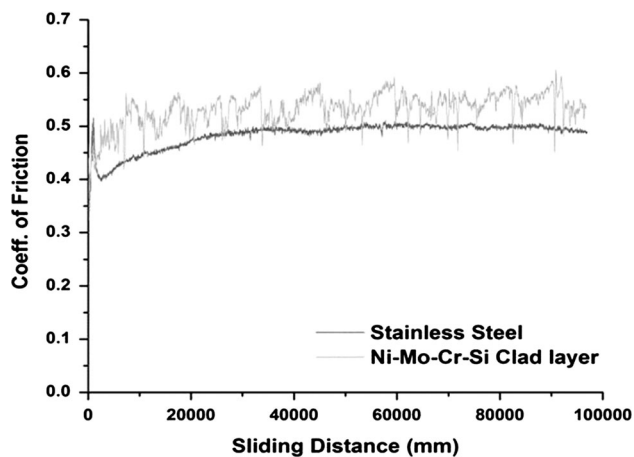


Fig. 12—Coefficient of friction vs sliding distance for the Ni-Mo-Cr-Si laser clad layer and SS316L substrate sliding against WC ball (5 N, 20 mm/s).

speeds (Figures 16(b), (c)). The discontinuous oxide clusters were also observed at a few locations of the track (Figure 16(d)).

Thus, mild wear mechanisms such as microploughing and oxidative wear were the dominant mechanism in sliding wear of clad layer at low loads and low speeds, whereas the wear mode of the clad layer was oxidation and microcracking at higher load and sliding speeds.

IV. DISCUSSION

Optimization of the laser cladding parameters resulted in defect free and metallurgically bonded clad layer of Ni-Mo-Cr-Si alloy with low dilution on SS316L substrate. Higher hardness of the clad layer can be attributed to the dispersion of hard intermetallic Mo-rich Laves phase in softer Ni-based gamma solid solution or eutectic mixture of both.^[9,10]

While sliding against 52100 Cr steel ball (under adhesive wear regime), SS316L substrate exhibited 4 to 5 times higher wear rate than that of the laser clad layer in all the test conditions. The dominant wear mechanisms in case of SS316L substrate were adhesive as well as oxidation and consequent detachment of the layer. Such adhesive mechanism of wear can result in yielding and plastic shearing^[25,26] as the actual contact stress at the asperities is significantly higher than the apparent or nominal contact stress due to roughness of any real surface. The detachment of material, fracture coupled with material loss may be due to extensive repeated plastic shearing resulting from adhesive phenomenon or brittle fracture with cracks initiated because of hertzian or tensile stress on the surface. Fracture generally occurs inside the surface having lower hardness as hardness is connected to local yield strength and results in direct wear loss on the softer surface. Navas *et al.*^[26] have reported the plastic deformation and oxidation of the wear track in case of 1045 Carbon steel which is expected to behave in a similar manner to stainless steel. Wear mechanisms of adhesive wear, brittle fracture, and

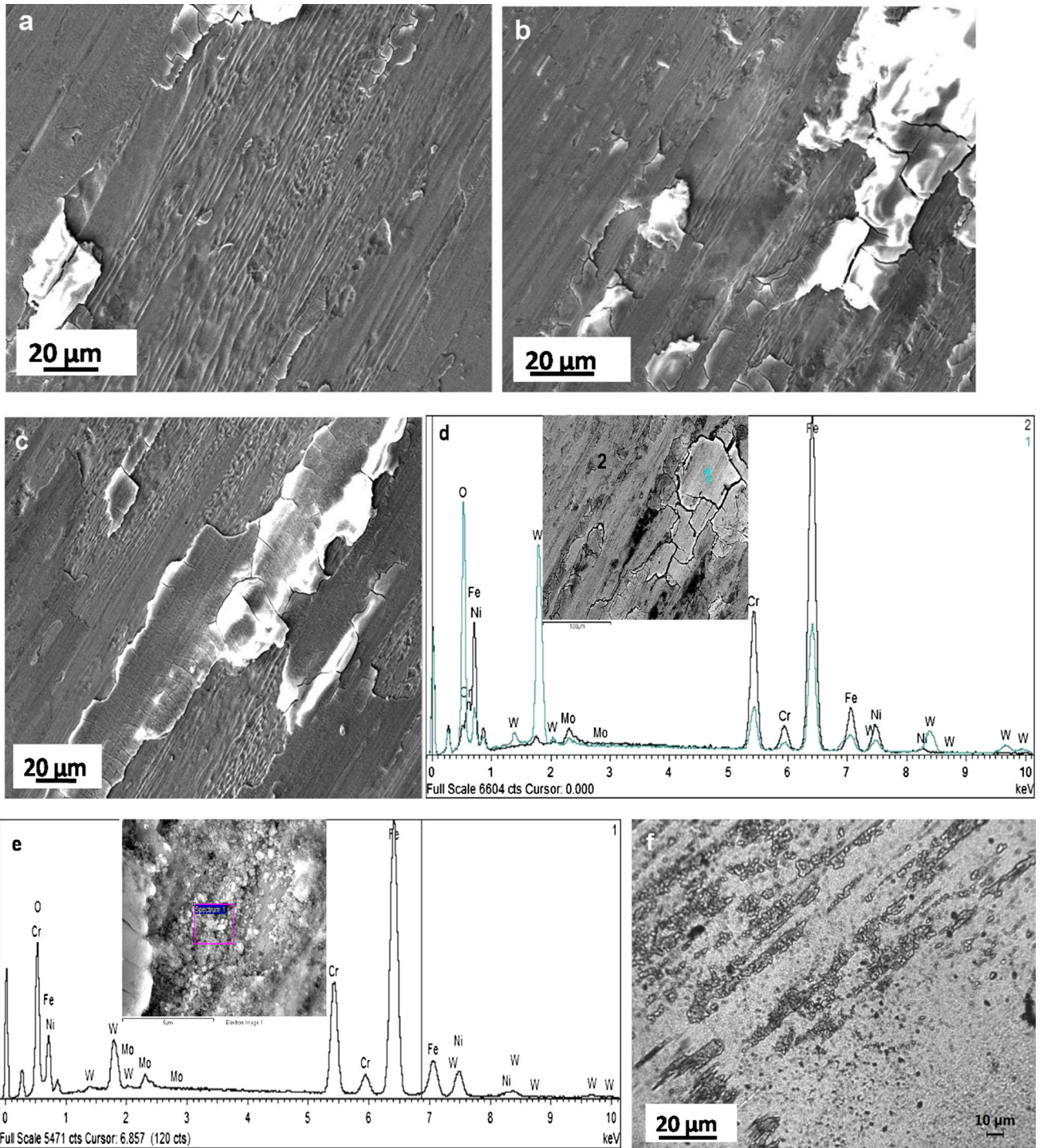


Fig. 13—SEM micrographs showing the morphology of the middle of wear track of the substrate SS316L under different loads (constant speed 20 mm/s) sliding against WC ball (*a*) 3 N (*b*) 5 N (*c*) 7 N and (*d*) BSE image and EDS microanalysis of the wear track (*e*) wear debris and EDS microanalysis (*f*) wear track of the ball.

oxidation were not present in case of the Ni-Mo-Cr-Si laser clad layer at low load and speed, which clearly explains much lower wear rate of the laser clad layer than the stainless steel substrate. Whereas at higher loads and speeds, more transfer of material from steel counterpart, its oxidation, consequent cracking and

material detachment resulted in increased wear rate. High velocity oxygen-fuel (HVOF)-sprayed Ni-Mo-Cr-Si coatings^[23] displayed considerable damage and large amounts of oxides (coming partly from the coating and partly from the steel counter body). Thus, qualitative wear characteristics (wear scar morphology) of the

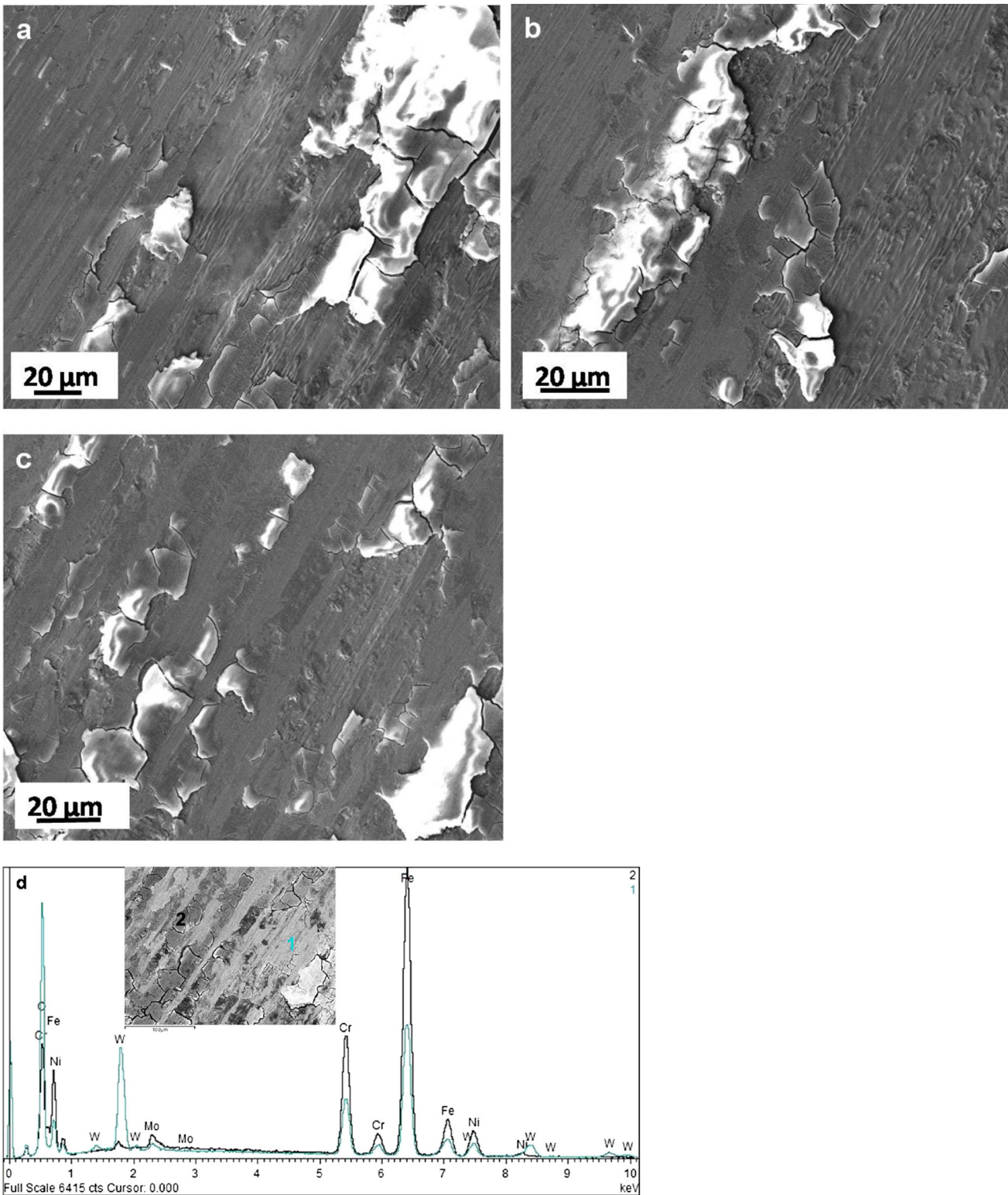


Fig. 14—SEM micrographs showing the morphology of the middle of wear track of the substrate SS316L under different speeds (constant load 5 N) sliding against WC ball (a) 20 mm/s (b) 40 mm/s (c) 60 mm/s (d) BSE image and EDS microanalysis of the wear track.

as-sprayed HVOF Ni-Mo-Cr-Si coatings does not differ significantly with those of the laser-deposited coatings at higher load and speeds, although significant damage was not observed at low loads and speeds in laser clad layer.

Quantitatively, the wear rate of the as-sprayed HVOF Ni-Mo-Cr-Si alloy was found to be higher than that of laser-deposited clad layer. However, because of different deposition processes, different sliding wear techniques

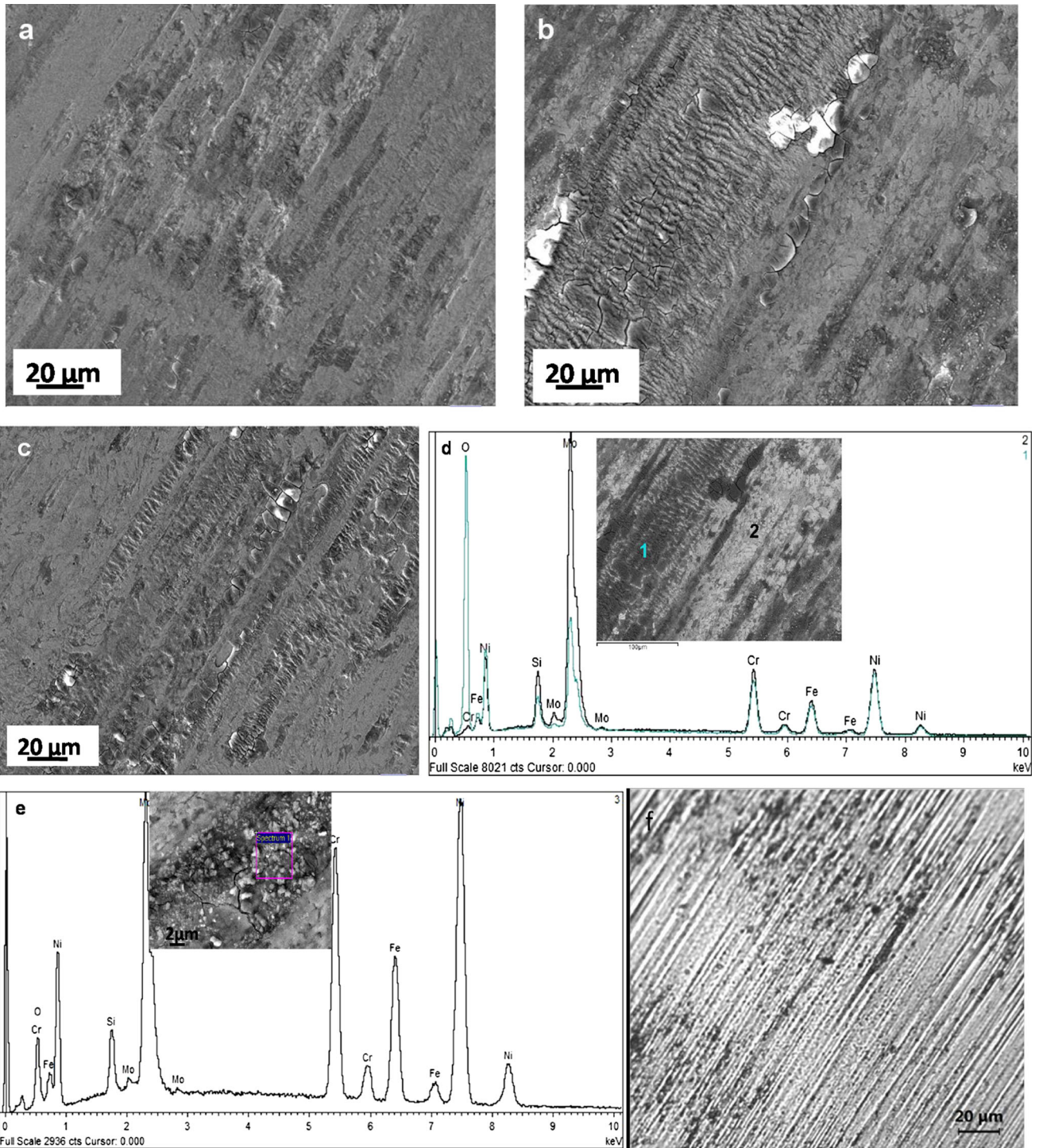


Fig. 15—SEM micrographs showing the morphology of the middle of wear track of the Ni-Mo-Cr-Si laser clad layer under different loads sliding against WC ball (*a*) 3 N (*b*) 5 N (*c*) 7 N and (*d*) BSE image and EDS microanalysis of the wear track (*e*) wear debris and EDS microanalysis present only at 7 N (*f*) wear track of the ball.

and conditions (loads, speeds) it is difficult to compare the wear characteristics (both qualitative and quantitative) of the laser-deposited Ni-Mo-Cr-Si clad with those of HVOF sprayed. The presence of oxide on wear track of other Co-based hardfacing alloys has also been reported.^[27,28] According to the criteria listed in,^[11] the wear resistance of Ni-Mo-Cr-Si laser clad layer exhib-

iting wear rate around 10^{-6} mm³/Nm sliding against 52100 Cr steel ball can be ranked excellent.

As hardness of 52100 Cr steel ball is higher (~850 VHN) than that of SS316L (~200 VHN), therefore, wear would have initiated by two-body mechanism and resulted in transfer of material. This could change the wear mode to three-body mechanism due to the wear

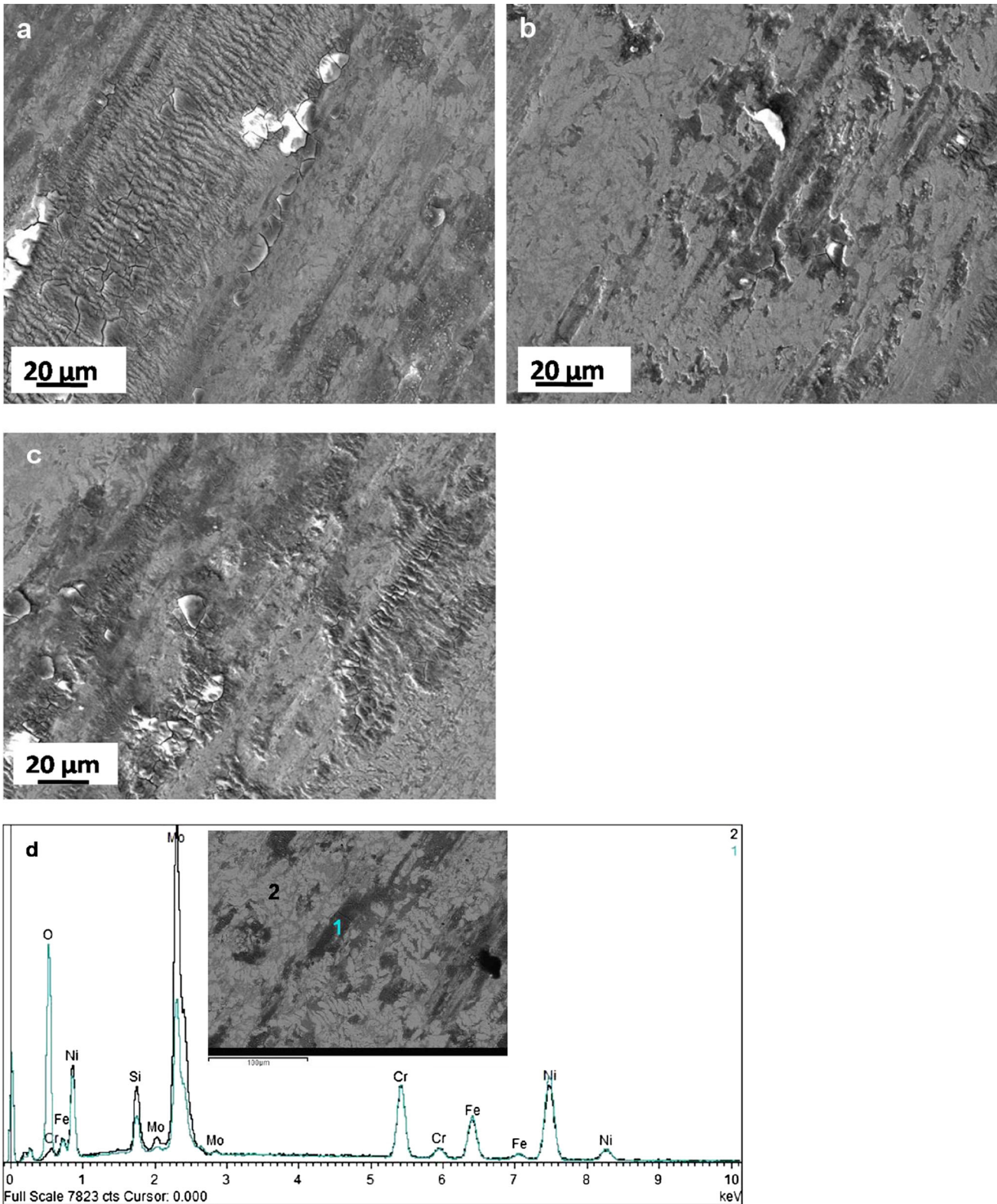


Fig. 16—SEM micrographs showing the morphology of the middle of wear track of the of the Ni-Mo-Cr-Si laser clad layer under different speeds sliding against WC ball (a) 20 mm/s (b) 40 mm/s (c) 60 mm/s (d) BSE image and EDS microanalysis of wear track.

particle trapped in the contact area. These plate-like particles may get trapped inside the wear track and undergo repeated yielding, crushing, and consequent

reduction in size to small rounded particles (Figure 7(f)). These small particles may undergo strong flash heating^[29,30] because of frictional heat generated during

repeated sliding wear and results in oxidation of the wear track. Additionally, the flash temperature at the asperities (contact time few microsecond) may be much higher than the equilibrium bulk temperature of the bodies. Thus, the asperities, transfer film, and crushed wear particles may attain critical oxidation temperature even if the bulk temperature is much lower and causes oxidation. The same mechanism of more material transfer, resulting oxidation and material loss holds true for clad layer at higher load and speed. The increase in flash heating with load and speed may also be responsible for oxidation at higher load and sliding speed in case of clad layer.

A slightly lower coefficient of friction in case of SS316L than that of clad layer sliding against 52100 Cr steel ball was due to formation of wear debris and its oxidation in contact area. These wear debris and oxide layer (rich in chromium oxide) in case of stainless steel provide more lubricating effect. Slight increase in COF with increased load may be attributed to the accumulation of wear debris and their entrapment and agglomeration. Sudden increase in COF of clad layer at higher load may be due to increased growth of transferred film and hence higher chemical affinity and adhesion.

Thus, the dominant wear mechanism of adhesive wear and plastic deformation in case of the stainless steel substrate sliding against the 52100 Cr steel ball is due to its lower hardness and therefore lower yield strength and higher plastic deformability. Such adhesive phenomena were absent in case of the Ni-Mo-Cr-Si laser clad layer due to higher hardness in all the contacting conditions. The brittle fracture was also absent during sliding against 52100 Cr steel at low load and sliding speed which indicated higher resistance to cracking due to dispersion of hard Laves phase in softer gamma solid solution phase. Although at higher loads and sliding speed, increased transfer of material from the steel counterpart and its oxidation and consequent delamination of oxide layer may be responsible for the brittle material detachment.

While sliding against WC ball counterpart, because of lower chemical affinity between the metallic coating as well as substrate and the ceramic ball and also because of high hardness of WC ball adhesive wear reduces, abrasive wear is favored. SS316L substrate was worn mainly by abrasion due to much harder WC ball. The extent of abrasive wear as well as transfer of the material was reduced in the clad layer as compared to those in SS316L due to higher hardness and hence enhanced load support. At higher load and sliding speed, the extent of deformation increased and the resulted strain hardening might have induced microcracking in the clad layer. This microcracking may be due to the presence of very few slip systems in hard intermetallic laves phases present in the Ni-Mo-Cr-Si systems. Thus, both plastic deformability and higher hardness are important for abrasive wear resistance. The oxidations of the wear track in both SS316L substrate and the Ni-Mo-Cr-Si laser clad layer, in all contacting conditions, were due to frictional heat generated during the dry sliding wear against much harder WC ball.

Under the oxidative wear regime, the improvement or degradation of the wear resistance is mainly controlled by kinetics of the oxide layer formation, properties, and its adherence to the surface. Thus, the wear debris and the oxide layer play dual role. It may control the friction and wear by preventing the direct contact of the surfaces and also by exerting lubrication effect. It may also act as an abrasive particle and cause abrasive wear. So, the wear process is also governed by particulate nature of the wear debris and its possibility of ejection or retention within the contact area. In small amplitude reciprocating motion, this wear debris is difficult to be pulled out and therefore contributes significantly to the wear process.

Embedded wear particles also play crucial role in wear of the counter body in case of abrasive wear regime. Wear particles get detached during the initial interaction of the asperities and get embedded in the relatively softer matrix. In case of the clad layer (which is relatively harder than substrate), these embedded wear particles caused microgrooving of the ball surface (Figure 15(g)).

Coefficient of friction of clad surface and substrate is much higher while sliding against WC ball as compared to that while sliding against 52100 Cr steel ball due to surface delamination and embedment of small wear debris produced by the abrasive processes (enriched in tungsten carbide and oxygen). Moreover, much lower thermal conductivity of WC ball favors higher flash temperatures than that in case of the 52100 Cr steel ball. High flash temperature is the reasons for oxidation even at lower loads and speeds. At higher load, the brittle fracture resulted in the form of microcracking hence some of the energy is dissipated, slightly reducing COF at higher loads. The oscillations in the coefficient of friction in case of the clad layer may be attributed to the presence of two different phases with different hardnesses^[10] as well as microcracking which resulted continuous and periodical forming and breaking of contact.

Thus due to higher hardness, the Ni-Mo-Cr-Si laser clad layer exhibited improvement in both adhesive and abrasive wear resistance as compared to the reference SS316L substrate. However, the improvement in the wear resistance of the clad layer as compared to the substrate was much more while sliding against 52100 Cr steel than that while sliding against WC, at the same contact stress intensity. Morphology of the wear track of both materials sliding against WC ball displayed noticeable differences. In any application involving wear of materials, not only the rate of removal of material, but also the surface conditions play an important role in selection of material. Therefore, the Ni-Mo-Cr-Si clad layer exhibited better wear resistance and surface conditions more specifically at lower loads and speed condition than SS316L substrate under the test conditions studied.

V. CONCLUSIONS

The optimization of the laser cladding parameters resulted in metallurgical bonded and defect-free clad

layer of Ni-Mo-Cr-Si with low dilution, on the stainless steel 316L substrate. The microstructure of the clad layer was primary dendrites of Mo-rich Laves phase dispersed in a relatively softer Ni-rich gamma solid solution or eutectic phase mixture. The hardness of the clad layer was much higher (~700 VHN) than that of stainless steel substrate (~200 VHN).

The Ni-Mo-Cr-Si laser clad layer exhibited higher wear resistance as compared to the SS316L substrate, sliding against both the counterparts (52100 chromium steel and WC ball). However, the improvement in the wear resistance of the clad layer as compared to that of the substrate was much more while sliding against 52100 Cr steel than that while sliding against WC ball. While sliding against 52100 Cr steel ball, combined wear mechanism of adhesion and plastic deformation, oxidation, and consequent detachment of material dominated the wear of stainless steel substrate, whereas in case of clad layer the wear was caused mainly by mild wear mechanism of small deformation at lower loads and speed and oxidation and microcracking at higher loads and speeds. While sliding against WC ball, stainless steel was worn mainly by abrasion, oxidation, and consequent cracking and delamination under all the wear test conditions. While mild wear mechanisms such as microploughing and oxidative wear were the dominant mechanism in sliding wear of the laser clad layer under the lower loads and speeds and the wear mode of the clad layer changed to oxidation and microcracking at higher loads and speeds.

REFERENCES

1. A. Frenk and W. Kurz: *Mater. Sci. Eng. A*, 1993, vol. 173, pp. 339–42.
2. A. Tiziani, L. Giordano, P. Matteazzi, and B. Badan: *Mater. Sci. Eng.*, 1987, vol. 88, pp. 171–75.
3. S. Atamert and H.K.D.H. Bhadeshia: *Metall. Trans. A*, 1989, vol. 20A, pp. 1037–53.
4. A.F.M. Arif and B.S. Yilbas: *J. Mater. Eng. Perfor.*, 2008, vol. 17, pp. 644–50.
5. R.D. Schmidt and D.P. Ferriss: *Wear*, 1975, vol. 32, pp. 279–89.
6. J.R. Devis: *Nickel, Cobalt and Their Alloys*, ASM International, Materials park, 2000.
7. A. Halstead and R.D. Rawlings: *Met. Sci. Technol.*, 1984, vol. 18, pp. 491–500.
8. S.E. Mason and R.D. Rawlings: *Mater. Sci. Technol.*, 1989, vol. 5, pp. 180–85.
9. R. Awasathi, S. Kumar, D. Srivastava, and G.K. Dey: *Pramana-J. Phys.*, 2010, vol. 75, pp. 1259–66.
10. R. Awasthi, S. Kumar, K. Chandra, B. Viswanadh, R. Kishore, C.S. Viswanadham, D. Srivastava, and G.K. Dey: *Metall. Mater. Trans. A*, 2012, vol. 43A, pp. 4688–4702.
11. Z.A. Foroulis: *Wear*, 1984, vol. 96, pp. 203–18.
12. T.A. Wolfla and R.C. Tucker: *Thin Solid Films*, 1978, vol. 53, pp. 353–64.
13. J. Vikstrom: *Wear*, 1994, vol. 179, pp. 143–46.
14. E.K. Ohriner, T. Wada, E.P. Wehlan, and H. Ocken: *Metall. Trans. A*, 1991, vol. 22A, pp. 983–91.
15. J.J. Demo, Jr. and D.P. Ferriss: E.I. du Pont de Nemours and Company, Wilmington, DE, U.S. Patent, 1974.
16. S. Kumar and G.L. Goswami: *Laser Eng.*, 2006, vol. 16, pp. 305–15.
17. R.N. Johnson and D.G. Farwick: *Thin Solid Films*, 1978, vol. 53, pp. 365–73.
18. G.L. Goswami, S. Kumar, R. Galun, and B.L. Mordike: *Lasers Eng.*, 2003, vol. 13, pp. 1–12.
19. C. Navas, M. Cadenas, and J.M. Cuetos: *J. Damborenea Wear*, 2006, vol. 260, pp. 838–46.
20. J. Przybylowicz and J. Kusinski: *Surface Coat. Technol.*, 2000, vol. 125, pp. 13–18.
21. M.X. Yao, J.B.C. Wu, S. Yick, Y. Xie, and R. Liu: *Mater. Sci. Eng. A*, 2006, vol. 435, pp. 78–83.
22. G. Bolelli and L. Lusvarghi: *J. Therm. Spray Technol.*, 2006, vol. 15 (4), pp. 802–10.
23. G. Bolelli, V. Cannillo, L. Lusvarghi, M. Montorsi, F.P. Mantini, and M. Barletta: *Wear*, 2007, vol. 263, pp. 1397–416.
24. B. Bhushan: *Principles and Applications of Tribology*, Wiley, New York, 1999, pp. 479–585.
25. G.W. Stachowiak and A.W. Batchelor: *Engineering Tribology*, 2nd ed., Butterworth Heinemann, Boston, 2001, pp. 533–52.
26. C. Navas, A. Conde, M. Cadenas, and J. de Damborenea: *Surf. Eng.*, 2006, vol. 22, pp. 26–34.
27. M.K. Stanford and V.K. Jain: *Wear*, 2001, vol. 251, pp. 990–96.
28. J.-N. Aoh and J.-C. Chen: *Wear*, 2001, vol. 250, pp. 611–20.
29. M.F. Ashby, J. Abulawi, and H.S. Kong: *Tribol. Trans.*, 1991, vol. 34 (4), pp. 577–87.
30. B. Bhushan: *Principles and Applications of Tribology*, Wiley, New York, 1999, pp. 431–78.